Journal of Engineering and Technological Advances (JETA)
https://jeta.segi.edu.my/index.php/segi
2023 Vol. 8 No. 2

PREPARING A MAP OF HIGH-POTENTIAL AREAS FOR GROUNDWATER RECHARGE IN NEYSHABUR PLAIN

[1]Hajian, F.*

Department of Civil Engineering, Neyshabur Branch, Islamic Azad University, Neyshabur, Iran.

* Corresponding Author: f.hajian@yahoo.com TEL: (+98)-912-8395641

Abstract: Most water is obtained from groundwater in dry and semi-dry regions when permanent water sources like rivers and lakes do not exist. It is vital that groundwater is recharged to ensure that it remains abundant. By utilizing remote sensing techniques, geographic information system, analytical hierarchy process, and considering seven layers, this article presents a method for identifying suitable groundwater recharge areas. The mentioned layers include rainfall maps, slope, land cover, soil texture, lithology, drainage network density, and lineament density of Neyshabur Plain with an area of 7134 square kilometers. The artificial recharge map of Neyshabur Plain was created with four suitable categories: excellent, good, moderate, and poor. According to the study, 5.8% and 69.9% of the study area would be excellent and good for artificial recharge, respectively, while 21% and 3.3% of the area would be poor and unsuitable for artificial recharge, respectively. Most areas with excellent to good recharge have a slope between 0 to 3.4 degrees and are used for irrigated agriculture, dry farming, and low-density pastures. The main soil type in areas with excellent to good recharge is loam followed by sandy loam. Validation was done with 56 piezometers throughout the study area. In addition, the relative operating characteristic curve (ROC) was performed which indicates a good prediction accuracy.

Keywords: suitable areas for groundwater recharge; remote sensing; geographic information system; analytical hierarchy process; artificial recharge map

1. Introduction

Groundwater resources provide nearly 22% of the world's water supply for domestic purposes, 9% for industrial activities, and 69% for irrigated agriculture (The United Nations Development Programme, 2022). Unfortunately, due to excessive exploitation of this natural resource, it has become a challenge in arid and semi-arid regions such as the Middle East where water demand for

various purposes like domestic, industrial, and agricultural has increased significantly in recent decades. Overuse of groundwater leads to several problems such as declining water table levels, pollution of the water and degradation of water quality and land subsidence. To solve these problems, there is an urgent need for management of groundwater resources (Singh *et al.*, 2017, Nag and Ghosh, 2013). Identifying important areas for groundwater recharge is essential for planning to reduce the decline in groundwater levels. There are several factors that influence groundwater movement in a region, such as rainfall, slope, land cover, soil texture, lithology, drainage density, and lineament density maps (Etikala *et al.*, 2019, Mishra *et al.*, 2020, Mogaji and Omobude, 2017).

Surface and subsurface water can be estimated in large areas with the help of geographic information system (GIS) and remote sensing. Various methods have been used to prepare maps of important areas for groundwater recharge around the world, such as frequency ratio, certainty factor, fuzzy logic index, and analytical hierarchy process (AHP). In particular, AHP has been considered a useful approach for predicting groundwater (Thapa *et al.*, 2017; Al-Ruzouq *et al.*, 2019).

The Ministry of Energy in Iran uses very expensive methods to supply water to many areas. Building dams in a dry climate with high evaporation is one of them. Most of these dams have had catastrophic environmental effects, such as the loss of a large number of trees, agricultural lands, villages and ancient monuments in the region such as Gotvand dam, Chamshir dam and Khersan 3 dam. Another method that has been considered for water supply is the transferring and pumping of water from the Oman Sea and the Persian Gulf to the other cities in Iran. Groundwater recharge in Iran, which is a very low-cost method compared to the above-mentioned methods, has been neglected. The aim of this article is to use GIS, remote sensing, and AHP techniques to map suitable areas for groundwater recharge in Neyshabur Plain.

2. Materials and Methods

2.1. Case Study

Neyshabur Plain is located between the geographical latitude of $N35^{\circ}40'$ to $N36^{\circ}39'$ and longitude of $E58^{\circ}17'$ to $E59^{\circ}30'$. It is situated in the northeast of Iran and has a semi-arid climate to arid climate. The area of the catchment is 7133.5 km^2. **Figure 1** shows the boundary of the Neyshabur Plain. The lowest point of the plain (Hoseinabad Jangal; outlet of the catchment) is at an altitude

of 1050 m above sea level, and the highest point is at 3300 m above sea level in the Binalud mountain range. The average annual rainfall is 234 mm. However, there is a variation for the annual rainfall from year to year. At the Mohammadabad Fadisheh station (in the plain area) and the Bar Arya station (in the hilly area), the average annual temperature is 13.8 and 13 °C, respectively. The potential annual evapotranspiration is about 2335 mm (Ahmadi *et al.*, 2013; Iran Chamber of Commerce, Industries, Mines and Agriculture, 2022). According to official reports, about 93.5% of groundwater in Neyshabur Plain are used for agriculture, and most of which are used for irrigation (Ahmadi *et al.*, 2013; Iran Chamber of Commerce, Industries, Mines and Agriculture, 2022). Also, about 4.2 % of the total water consumption is obtained from surface water. This suggests that groundwater is the principal source of water for diverse uses compared to the surface water in the Neyshabur catchment (Ahmadi *et al.*, 2013).

For every meter decline in the groundwater level in the Neyshabur Plain, the electrical conductivity (EC), the total hardness, the concentration of chloride ions, the concentration of sulfate, and the sodium adsorption ratio (SAR) values increase by approximately 140 µmhos/cm, 19 mg/L, 0.5 mEq/L, 0.3 mEq/L and 0.32, respectively. This result clearly indicates that continued extraction of groundwater resources under current conditions can lead to salinization of the aquifer. Additionally, the land subsidence rate was found to be about 10.5 cm/year or about 13.5 cm/m of groundwater level decline (Iran Chamber of Commerce, Industries, Mines and Agriculture, 2022). Therefore, it is important to recharge groundwater in the Neyshabur Plain to prevent the groundwater salinity, groundwater level decline and land subsidence.

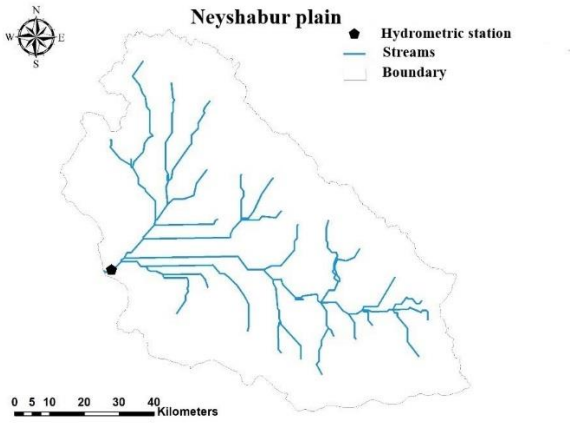

Figure 1. Boundary of the Neyshabur Plain

2.2. Data

The analysis was conducted based on eight factors to determine the best places for groundwater recharge: rainfall, slope, land cover, soil texture, lithology, drainage density, and lineament density maps. **Figure 2** shows the method used to determine suitable locations for groundwater recharge. First, a map of each parameter was prepared, and then each map was classified into five suitable classes (1-5): 5 (excellent), 4 (good), 3 (moderate), 2 (poor), and 1 (very poor and unsuitable), as shown in **Table 1** (Mahmoud, 2014). For each of the above parameters, greater rank values are given to classes that are more appropriate and crucial for finding groundwater recharge sites.

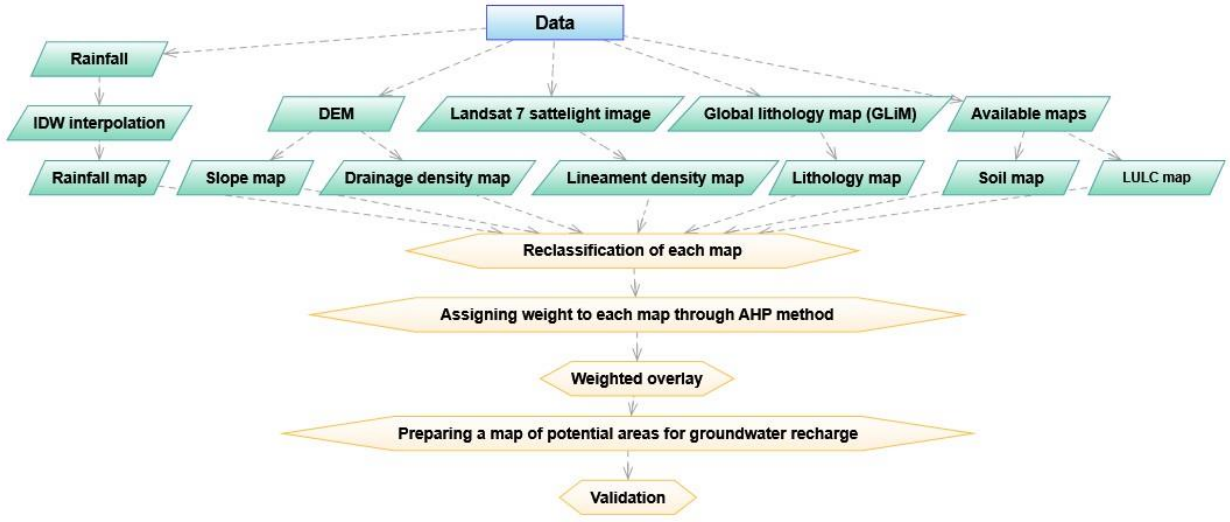

Figure 2. Flowchart of methodology for this study

2.3. Slope (SLO)

Slope is the change in heights between two points and directly affects the infiltration and groundwater recharge. The energy of the water flow is changed by the slope, so the slope and the infiltration rate are inversely related. In this study, digital elevation model (DEM) with a 30 m resolution was utilized to create the slope map using spatial analysis tool available in GIS (**Figure 3**). Then, the slope map was reclassified and ranked into five classes depending on the degree of infiltration of different slopes, as shown in **Table 1** (Mengistu *et al.*, 2022).

Table 1. Ranking of appropriate variables

Parameter	Range	Rank
Rainfall mm/month	79-95.7	1
	95.7-107.5	2
	107.5-123.9	3
	123.9-148.7	4
	148.7-185.9	5
Soil	Silty Clay	1
	Clay Loam, Sandy Clay Loam	3
	Silt Loam, Loam	4
	Sandy Loam, Loamy Sand, Sand	5
Lithology	Pb, pb-mt, vi , mt	1
	sc py	2
	ssmxcl	3
	sumxv, scshev, sc pu	4
	smmx, smmxev, smss, suss	5
Lineament density Km/km^2	0-0.34	1
	0.34-1.1	2
	1.1-2.1	3
	2.1-3.2	4
	3.2-4.9	5
Drainage density Km/km^2	0-5.1	5
	5.1-14.4	4
	14.4-24.9	3
	24.9-38.1	2
	38.1-60.7	1
slope (degree)	0-3.4	5
	3.4-9.5	4
	9.5-17.3	3
	17.3-26.2	2
	26.2-54.1	1
land use / land cover	(1) and (2)	1
	(3)	2
	(4) and (5) and (6)	3
	(7)	4
	From land use (8) to land use (14)	5

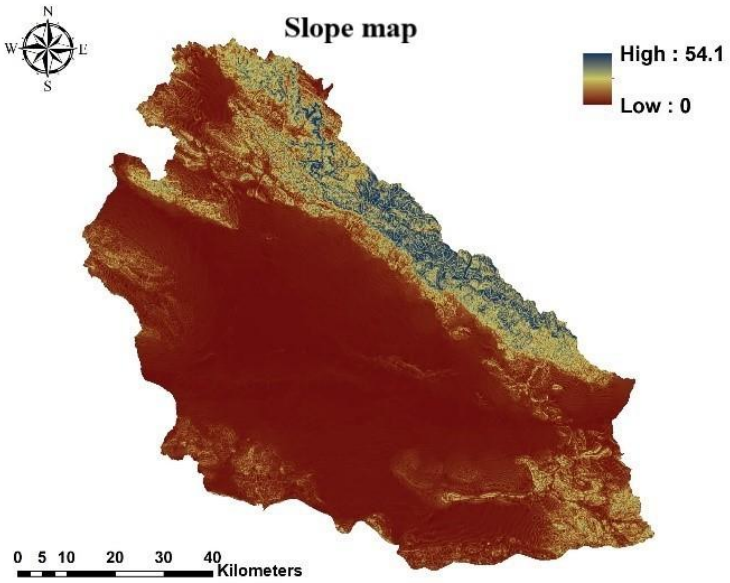

Figure 3. Slope map of Neyshabur Plain

2.4. Soil Factor (SL)

The infiltration of water into an aquifer in a region depends on the type of the soil, its depth and hydraulic conductivity. Because of the wider pore spaces between soil particles, sandy soils have greater hydraulic conductivity than finer-grained soils. Water infiltrates much more slowly in clayey soils than in sandy soils. The ability of various soil textures to absorb water differs (Wondim, 2016). The map obtained was classified into five main classes, as shown in **Table 1**. Previous study presented a table that provides the infiltration rate for different soil textures, the classification was made into five classes as well (Berhanu *et al.*, 2013). The soil map of Neyshabur Plain is presented in **Figure 4.** Soil map of Neyshabur Plain .

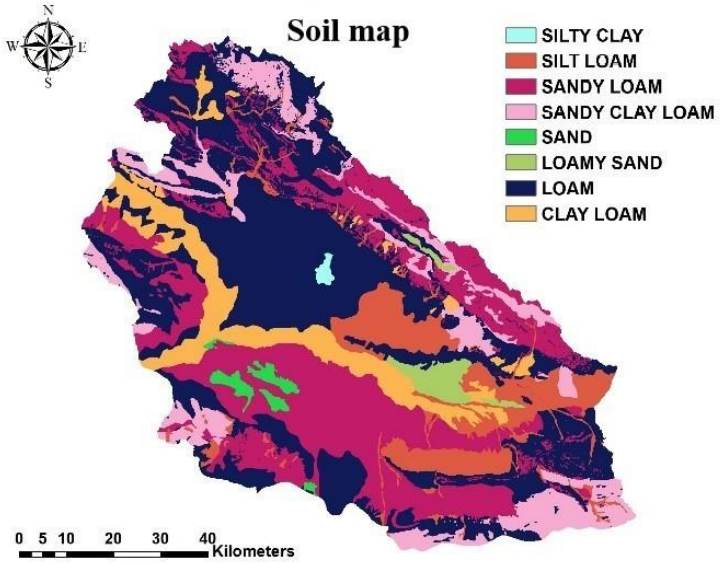

Figure 4. Soil map of Neyshabur Plain

2.5. Drainage Density (DD)

Drainage density refers to the proximity of stream networks. High drainage density will result in low groundwater recharge and vice versa. Drainage density is calculated using Line Density Tool and stream network map in Arc Map (Mengistu *et al.*, 2022). **Figure 5.** Drainage density map of Neyshabur Plain shows the drainage density map of Neyshabur Plain.

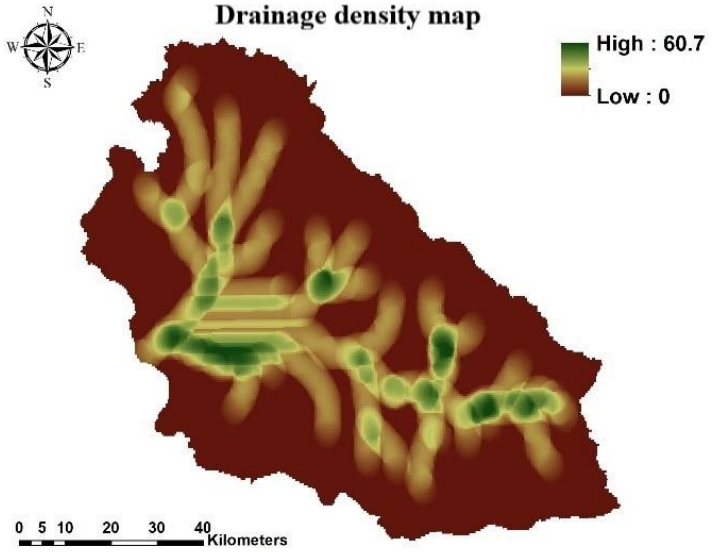

Figure 5. Drainage density map of Neyshabur Plain

2.6. Lineament Density (LD)

Underground fractures and faults increase infiltration rate and groundwater recharge. Higher water infiltration rates are usually associated with areas with high lineament density and vice versa. Landsat 7-ETM+ panchromatic band with a resolution of 15 m (downloaded from EarthExplorer.usgs.gov) and lineament extraction section in PCI Geomatica 2017 software and also the Line Density Tool in Arc Map were used to create the Lineament density map of the region (Uc Castillo *et al.*, 2022). The lineament density map of Neyshabur Plain is showned in **Figure 6.** Lineament density map of Neyshabur Plain .

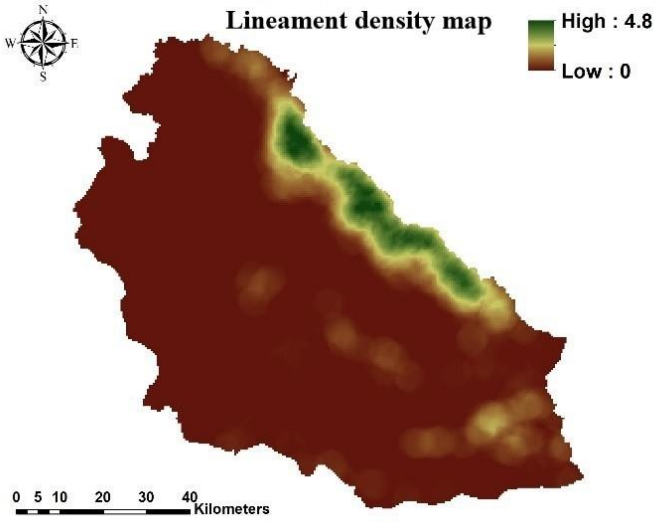

Figure 6. Lineament density map of Neyshabur Plain

2.7. Lithology (LI)

Lithology actually affects the permeability of water flow and controls the groundwater recharge. Previous study has provided the global lithology map (GLiM) using 1,235,400 polygons collected from 92 regional geological maps and additional research records (Hartmann and Moosdorf, 2012). The high resolution of GLiM provides the possibility of observing regional lithology or geological distributions. A gridded version of GLiM is accessible in the PANGEA database (*http://dx.doi.org/10.1594/PANGAEA.788537*), and the original GIS data can be downloaded through this link (*https://www.dropbox.com/s/9vuowtebp9f1iud/LiMW_GIS%202015.gdb.zip?dl=0*). Lithology map of Neyshabur Plain was extracted from the above map. The rocks present in **Figure 7** are explained in **Table 2**. The lithology map is classified in five categories (**Table 1**) based on the

permeability index (Widodo *et al.*, 2017) or hydraulic conductivity (Ku *et al.*, 2009) of different rocks.

Table 2. Explanation of lithology and available rocks in Neyshabur Plain

Explanation	Lithology
Plutonic rock with very low permeability	Pb
Combination of metamorphic and plutonic rock with very low permeability	Pb-mt
Carbonated rocks such as limestone and dolomite	Scpu
Pyroclastic carbonate stones that are heavily weathered	Scpy
Carbonate rocks with smaller particles than fine dominant sand	Scshev
Sedimentary rocks with mixed particles, usually a combination of various types of rocks (such as sandstone and limestone).	Smmx
Sedimentary rocks with mixed particles, usually a combination of various types of rocks (such as sandstone and limestone) that have been slightly weathered.	Smmxev
Sedimentary rocks containing coarse-grained particles (with coarse grains being dominant) .	Smss
Siliciclastic sedimentary rocks, such as sandstone and mudstone, examples of sedimentary rocks. .	Ssmxcl
Young, unconsolidated sedimentary deposits, combination of particles of all sizes, such as sand dunes and alluvial deposits (Alluvial deposits).	Sumxv
Young, unconsolidated sedimentary deposits containing coarse-grained particles.	Suss
Medium volcanic rocks, usually Andesites	Vi
Metamorphic rocks like shale with very low permeability	mt

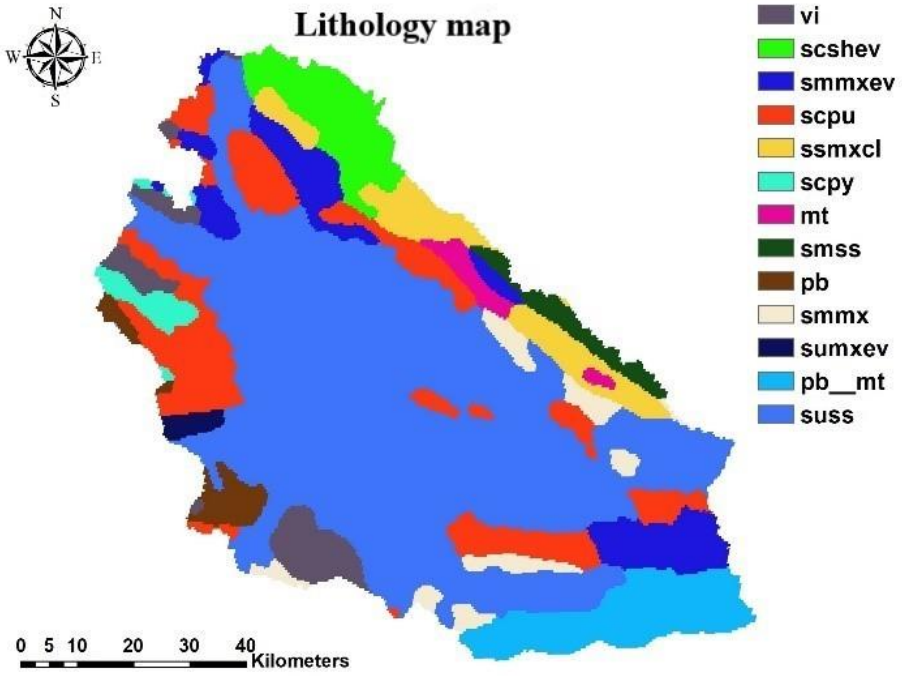

Figure 7. Lithology map of Neyshabur Plain

2.8. Rainfall (RN)

The rainfall data was available for April 2008 from Tamab (Water Resources Research Organization in Tehran) for 11 rain gauge stations (April had the highest rainfall in that year). The average rainfall for the study area in April 2008 was about 108 mm. Clearly, the more rainfall will lead to higher groundwater recharge. The precipitation map was created in Arc Map using the inverse distance weight interpolation technique. The resulting map was classified into five main classes (**Table 1**). The rainfall map of Neyshabur Plain for year 2008 is presented in **Figure 8.** Rainfall map of Neyshabur Plain for year 2008 .

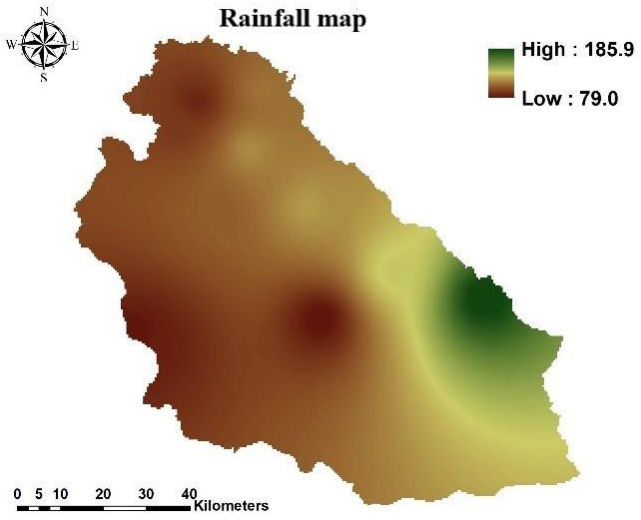

Figure 8. Rainfall map of Neyshabur Plain for year 2008

2.9. Land use / land cover (LULC)

Land use has great impact on infiltration and groundwater recharge. The land use and land cover map with a resolution of 30 m was obtained from the natural resources of Neyshabur for the year 2008. The land use and land cover map are classified into aquifer recharge categories based on the degree of infiltration of different land uses and covers. The following areas are numbered as shown in **Table 1**: residential and industrial areas (1), sand dunes and alluvial fans (2), dense pastures (3), rocky mass lands without vegetation (4), semi-dense pastures (5), alluvial bed deposits (6), sparse pastures (7), dry farming (8), natural forests (9), irrigated farming (10), irrigated orchards (11),

water surfaces (12), planted forests (13), and shrublands (14). The ranks and ratings given in **Table 1** were based on the previous study (Uc Castillo *et al.*, 2022). **Figure 9** shows the land use map of of Neyshabur Plain for Year 2008.

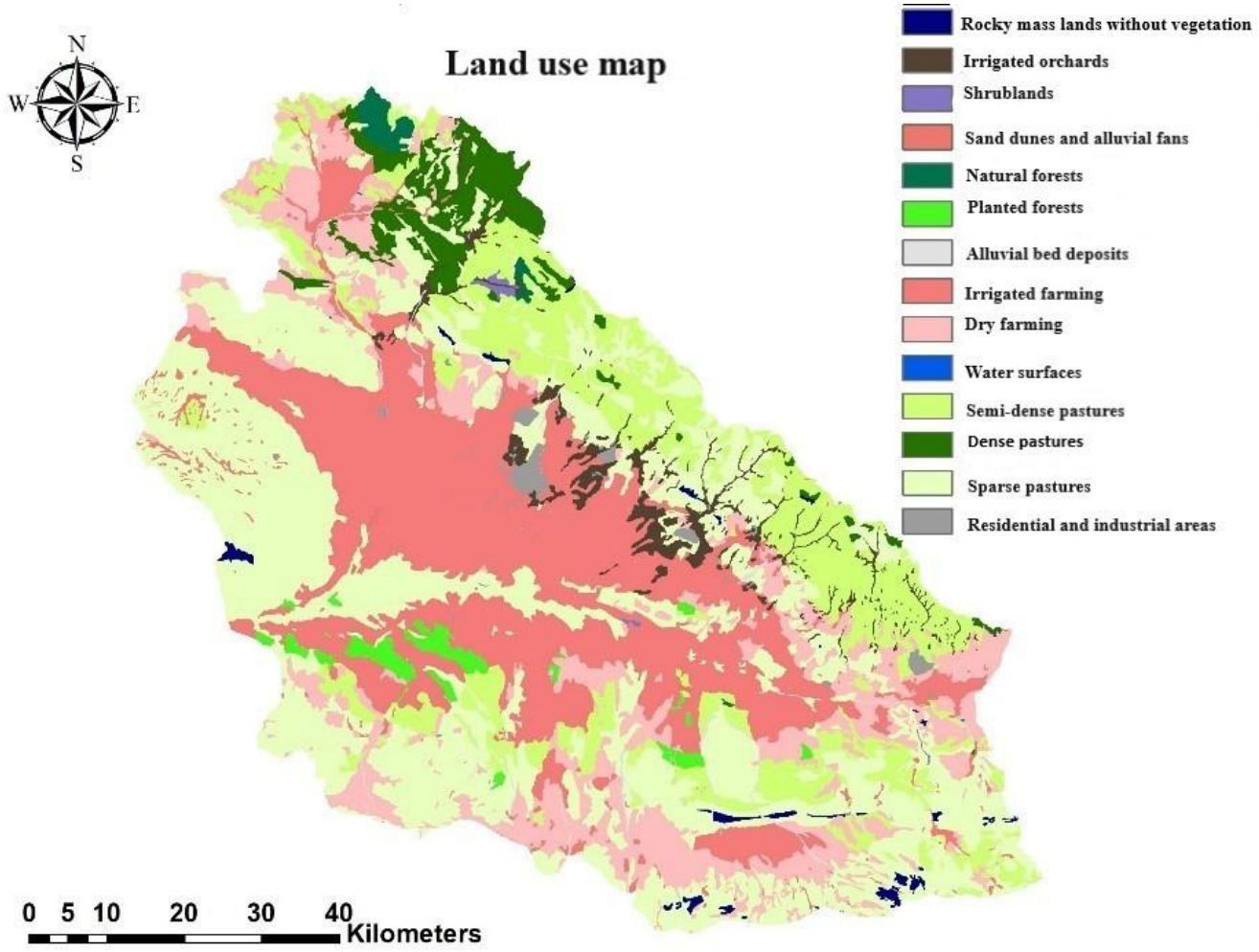

Figure 9. Land use map of of Neyshabur Plain for Year 2008

2.10. Analytical Hierarchy Process

In AHP, different thematic layers and their associated features were weighed according to a complex multi-criteria decision-making method. Delineating groundwater recharge zones in the study area was done in four stages using this method: (1) identifying factors that affect groundwater recharge, (2) creating pairwise comparison matrix, (3) relative weight estimation, and (4) matrix consistency evaluation. The description of this method is based on the previous studies in the literature (Uc Castillo *et al.*, 2022; Zghibi *et al.*, 2020).

2.11. Selection of Factors Affecting Groundwater Recharge

Groundwater recharge factors were first scored between 1 and 9 according to their importance in pairwise comparisons with other factors in the AHP. For this purpose, scores of 1-9 were used, as shown in **Table 3** (Saaty, 2001). This score describes the relative impact of parameters, with a score of 1 indicating equal impact, and a score of 9 indicating a severe impact of one parameter on groundwater recharge, as shown in **Table 4** in the following section.

Table 3. Scores of the analytic hierarchy process based on Saaty, 2001

Importance	Equal importance	Moderate importance	Strong importance	Very strong importance	Extreme importance	Intermediate values between the two adjacent judgments
Score	1	3	5	7	9	2,4,6,8

2.12. Pairwise Comparison Matrix

Comparing the first element of this matrix to itself, it received a score of 1 (**Table 4**). When comparing more influential parameters with less influential parameters, the rows were filled using scores from the previous study (Saaty, 2001) and inverse the scores when comparing less influential parameters with more influential parameters. The pairwise comparison matrix for the parameters investigated in this study is shown in **Table 4**. The first parameter in the matrix was chosen as lithology because it has a bigger effect on groundwater recharge than other components. As a result, lithology was assigned a value of 8 in comparison to soil. And based on the importance of parameters in groundwater recharge, all parameters were placed in the next positions. The scoring in **Table 4** was based on the study from the literature (Uc Castillo *et al.*, 2022).

Table 4. Pairwise comparison matrix

Parameter	LI	LULC	SLO	LD	RN	DD	SL
LI	1	2	3	5	6	7	8
LULC	0.50	1	2	4	5	6	7
SLO	0.33	0.50	1	3	4	5	6
LD	0.20	0.25	0.33	1	2	3	4
RN	0.17	0.20	0.25	0.50	1	2	3
DD	0.14	0.17	0.20	0.33	0.50	1	2
SL	0.13	0.14	0.17	0.25	0.33	0.50	1

Sum of each column	2.47	4.26	6.95	14.08	18.83	24.50	31.00

2.13. Estimation of Relative Weight

The weight was obtained by normalizing the pairwise comparison matrix, as shown in **Table 5**. The elements of the normalized pairwise comparison matrix is calculated by dividing the values of the components of the pairwise comparison matrix by the summation of the corresponding column. Next, the standard weight for each layer or parameter (AHP weight shown in **Table 5**) is calculated by averaging all normalized pairwise comparison matrix elements in each row.

Table 5. Normalized pairwise comparison matrix

Parameter	LI	LULC	SLO	LD	RN	DD	SL	AHP Weight
LI	0.41	0.47	0.43	0.36	0.32	0.29	0.26	0.361
LULC	0.20	0.23	0.29	0.28	0.27	0.24	0.23	0.249
SLO	0.14	0.12	0.14	0.21	0.21	0.20	0.19	0.174
LD	0.08	0.06	0.05	0.07	0.11	0.12	0.13	0.088
RN	0.07	0.05	0.04	0.04	0.05	0.08	0.10	0.060
DD	0.06	0.04	0.03	0.02	0.03	0.04	0.06	0.040
SL	0.05	0.03	0.02	0.02	0.02	0.02	0.03	0.028
Sum	1	1	1	1	1	1	1	1

Next, the AHP weight of the corresponding variable from **Table 5** was multiplied by each column of the pairwise comparison matrix. The sum of the rows then gives the total weight value. Subsequently, the compatibility vector (λ value) was obtained by dividing the total weight value by the AHP weight of the required variable. λmax was obtained by taking the average of all λ, as shown in **Table 6**.

Table 6. Determining the compatibility vector

Parameter	LI	LULC	SLO	LD	RN	DD	SL	The sum of each row (total weight value)	Compatibility vector
LI	0.36	0.50	0.52	0.44	0.36	0.28	0.22	2.69	7.45
LULC	0.18	0.25	0.35	0.35	0.30	0.24	0.20	1.87	7.48
SLO	0.12	0.12	0.17	0.26	0.24	0.20	0.17	1.29	7.41
LD	0.07	0.06	0.06	0.09	0.12	0.12	0.11	0.63	7.18
RN	0.06	0.05	0.04	0.04	0.06	0.08	0.08	0.42	7.07
DD	0.05	0.04	0.03	0.03	0.03	0.04	0.06	0.28	7.05
SL	0.05	0.04	0.03	0.02	0.02	0.02	0.03	0.20	7.12

	$Average\ of\ last\ column = \lambda_{max}$	7.25

2.14. Evaluation of Matrix Compatibility

The compatibility index (CI) and compatibility ratio (CR) are used to assess compatibility.

$$CI = \frac{\lambda_{max} - n}{n - 1} = \frac{7.25 - 7}{7 - 1} = 0.0418 \quad (1)$$

$$CR = CI/RI \quad (2)$$

where n is the total number of parameters, which is 7, and RI was obtained from **Table 7** as 1.32. CR was also calculated to be 0.031. CR should be less than one; otherwise, the pairwise comparison matrix scores must be repeated (Uc Castillo *et al.*, 2022).

Table 7. Determining the value of RI based on the total number of parameters

n	**2**	**3**	**4**	**5**	**6**	**7**	**8**	**9**
RI	0	0.58	0.9	1.12	1.24	1.32	1.41	1.49

2.15. Preparing a Map of Potential Areas for Groundwater Recharge

Figure 10 shows the map of different groundwater recharge potentials. This map was obtained in Arc Map software using the weighted overlay command through the following formula:

$$GWPZs = \sum_{i=1}^{n} \sum_{j=1}^{m} (w_i \times x_j) \quad (3)$$

where w_i is the rank and order of parameters from **Table 1**, and x_j is the AHP weight of parameters from **Table 5**.

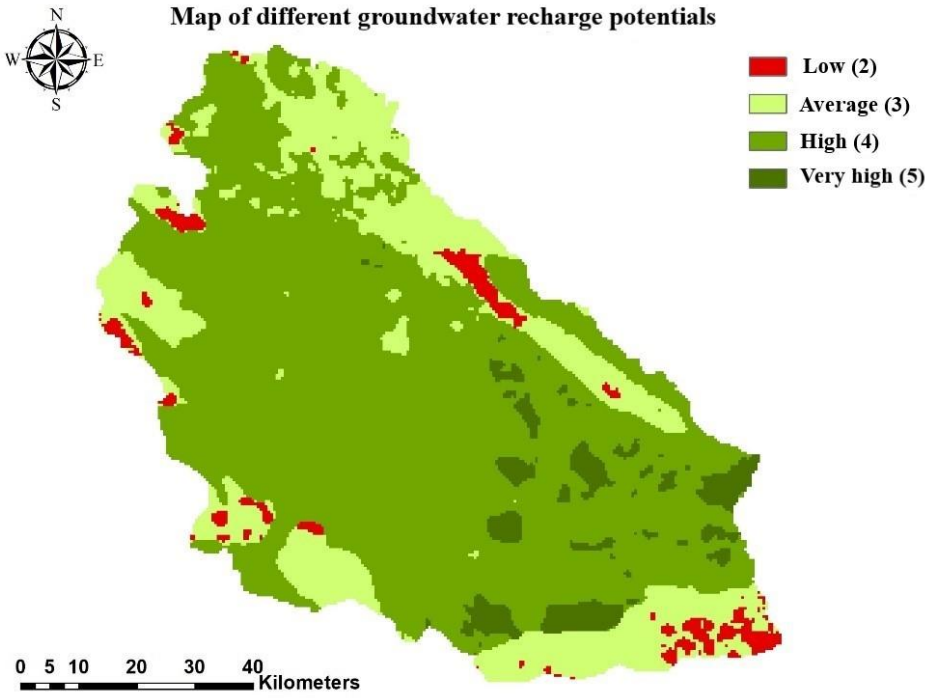

Figure 10. Map of different groundwater recharge potentials

3.0. Results and Discussion

3.1. Validation

Although the number of observed wells in the plain area is considerable, their density and distribution are not satisfactory. The biggest issue is in the southern, northern, and southeastern areas of the plain, where there are no observed wells. **Figure 11** shows that the underground water level decreases from the north, northeast, northwest and south towards the center of the aquifer. The maximum groundwater level is located in the southern and southeastern regions where the areas with very high groundwater recharge potentials are located, as shown previously in **Figure 10**. The relative operating characteristic curve (ROC) was also prepared in Arc Map software using Arc SDM tool by considering the existing piezometer locations as true positives and different groundwater recharge potentials as a classification method. **Figure 12** depicts the ROC generated by the AHP model [Area Under the Curve (AUC) = 0.905]. AUC values of 0.5-0.6, 0.6-0.7, 0.7-0.8, 0.8-0.9, and 0.9-1 are considered poor, average, good, very good, and excellent, respectively (Ahmadi *et al.*, 2020). Therefore, the AHP model used in this work shows reasonable accuracy in

predicting different potentials for groundwater recharge. However, the limitation for this research is the lack of sufficient number of piezometers in the whole of the aquifer.

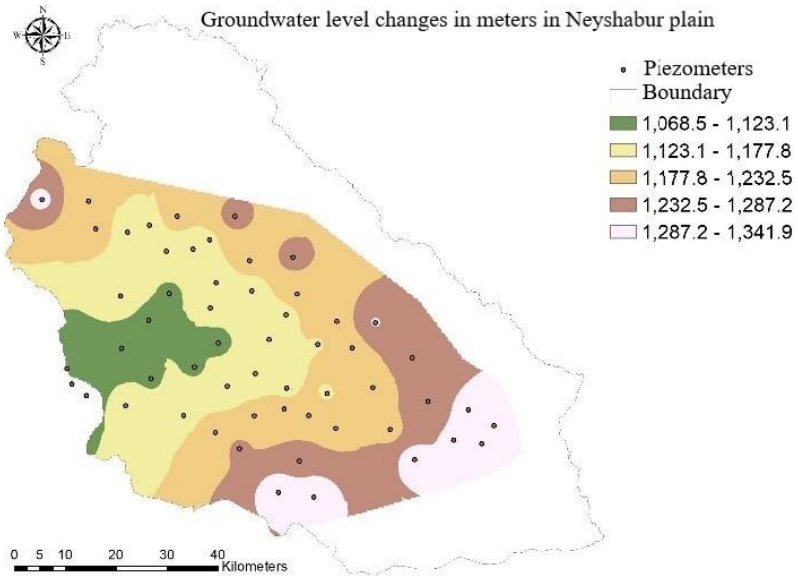

Figure 11. Map of groundwater level changes and available piezometers in Neyshabur Plain

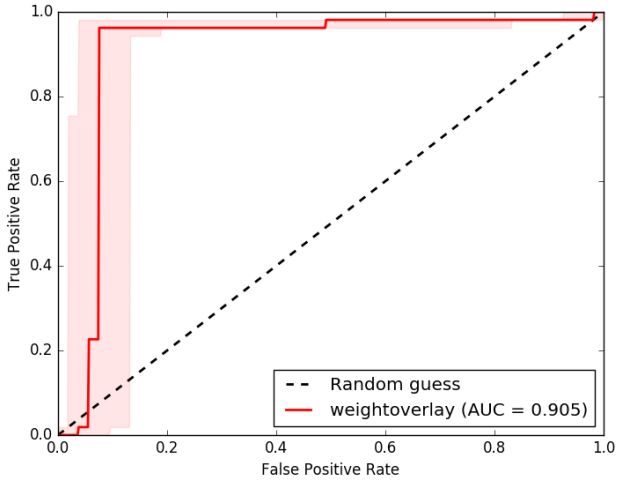

Figure 12. Produced relative operating characteristic curve using the analytical hierarchy process model

3.2. Discussion

As shown in **Table 8**, about 5.8% and 69.9% of the study area are classified as excellent and good for groundwater recharge, respectively, while 3.3% are classified as poor and unsuitable.

Table 8. Areas classified under different suitability categories

Suitability for artificial recharge	Area in square kilometers	Percentage of the total area of Neyshabur Plain	recharge-to-rainfall ratio (UN, 1967)
Excellent	411.1	5.8	47.5
Good	4985.9	69.9	32.5
Average	1499.2	21.0	15
Poor	237.2	3.3	7.5

The results show that 53.5% of the areas suitable for recharge have slopes ranging from 0 to 3.4 degrees, while 29.1% and 18.3% of the areas suitable for recharge are located on Loam and Sandy Loam soils, respectively. 47% of the areas suitable for recharge are located in areas with SUSS lithology (unconsolidated young deposits containing coarse particles). The area suitable for recharge is 22.4%, 24.1%, and 9.5% with low-density grazing (poor), irrigated agriculture, and rainfed agriculture, respectively. Areas with high permeability include the most permeable lithological units, gentle slopes, low drainage density, and soil layers with high infiltration capacity.

Determining the rate of groundwater recharge by direct measurement is difficult, and estimating it improves the understanding of hydrological processes at the catchment scale. Potential areas for groundwater recharge maps have been used for extracting rainfall-recharge ratio for the AHP method (**Table 8**). A simple estimate of the volume of water (W) infiltrated and recharged groundwater resources for the AHP method was calculated by multiplying the annual rainfall volume (P) by the recharge-to-rainfall ratio and the percentage of area. If the average rainfall for 2008 is considered as 301mm/year or 2147033000 m^3/year, then the amount of groundwater recharge in that year is equal to:

$$W_{AHP} = 2147033000 \times [(0.075 \times 0.033) + (0.21 \times 0.15) + (0.699 \times 0.325) + (0.058 \times 0.475)] = 619848427\ m^3/year$$

According to the present study, 28.8% (619848427 m^3/year) of the received precipitation in the study area infiltrates into the aquifers and recharges the groundwater, while the rest is lost through evaporation and transpiration or surface runoff. In 2008, the amount of water extracted by authorized and unauthorized wells in Neyshabur Plain was 681635266 m^3/year, indicating that

61786838 m^3/year of groundwater resources were overexploited in that year. Neyshabur Plain is being overexploited as a result of increased demand for irrigation, agricultural, residential and industrial activities in the study region. Artificial recharge solutions such as check dams, recharge basins, land flooding, and recharge wells can be employed to supplement the existing groundwater resources in the Neyshabur Plain. However, due to the high evaporation and transpiration rates in Neyshabur Plain, using recharge wells in areas with high-potential for groundwater recharge is likely to be more successful. Moreover, unauthorized well pumping from groundwater resources should be prevented.

4. Conclusion

The map of different potential areas for groundwater recharge shows that areas with good potential for recharge cover almost 70% of the entire plain, while areas with excellent potential cover almost 6% of the plain and are mainly concentrated in the eastern, northeastern, and southeastern parts of the study area. Areas with excellent potential for groundwater recharge are located on Sandy Loam and Silt Loam soils, rainfed and irrigated agriculture areas, and SUSS lithology (unconsolidated young deposits containing coarse particles) with slopes ranging from 0 to 3.4 degrees. It is crucial to note that these locations receive average to high rainfall (107-148 mm), demonstrating that lithology, land use, soil, and slope are more efficient in groundwater recharging than rainfall. Since the potential for groundwater recharge is directly related to percolation, the scores and ranks determined may be more accurate and objective if the infiltration and hydraulic conductivity of the entire area are measured locally. The map depicting several potential groundwater recharge regions can assist planners and engineers in improving groundwater resources and land use planning in the research area. Moreover, in addition to the issue of overexploitation of groundwater resources in Neyshabur plain, it is imperative to investigate the impact of climate change on groundwater resources for future studies.

Acknowledgement

The authors would like to thank Dr Bagher Zahabiyoun from Iran University of Science and Technology for supporting the research of this study.

Conflicts of Interest

The authors declare no conflict of interest.

References

Ahmadi, H., Kaya, O. A., Babadagi, E., Savas, T., & Pekkan, E. (2020). GIS-based groundwater potentiality mapping using AHP and FR models in central antalya, Turkey. *Environmental Sciences Proceedings*, 5(1), 11.

Ahmadi, T., Ziaei, A.N., Davary, K., Faridhosseini, A., Izadi, A., & Rasoulzadeh, A. (2013), Estimation of groundwater recharge using various methods in Neishaboor Plain, Iran. In *Groundwater Modeling and Management under Uncertainty*. Taylor & Francis Group.

Al-Ruzouq, R., Shanableh, A., Merabtene, T., Siddique, M., Khalil, M. A., Idris, A., & Almulla, E. (2019). Potential groundwater zone mapping based on geo-hydrological considerations and multi-criteria spatial analysis: North UAE. *Catena*, 173, 511-524.

Berhanu, B., Melesse, A. M., & Seleshi, Y. (2013). GIS-based hydrological zones and soil geo-database of Ethiopia. *Catena*, 104, 21-31.

Etikala, B., Golla, V., Li, P., & Renati, S. (2019). Deciphering groundwater potential zones using MIF technique and GIS: A study from Tirupati area, Chittoor District, Andhra Pradesh, India. *HydroResearch*, 1, 1-7.

Hartmann, J., & Moosdorf, N. (2012). The new global lithological map database GLiM: A representation of rock properties at the Earth surface. *Geochemistry, Geophysics, Geosystems*, 13(12).

Iran Chamber of Commerce, Industries, Mines and Agriculture. (2022). *Environmental effects caused by the reduction of water resources in the Neyshabur Plain*, report in Persian.

Ku, C. Y., Hsu, S. M., Chiou, L. B., & Lin, G. F. (2009). An empirical model for estimating hydraulic conductivity of highly disturbed clastic sedimentary rocks in Taiwan. *Engineering Geology*, 109(3-4), 213-223.

Mahmoud, S. H. (2014). Delineation of potential sites for groundwater recharge using a GIS-based decision support system. *Environmental Earth Sciences*, 72, 3429-3442.

Mengistu, T. D., Chang, S. W., Kim, I. H., Kim, M. G., & Chung, I. M. (2022). Determination of potential aquifer recharge zones using geospatial techniques for proxy data of Gilgel Gibe Catchment, Ethiopia. *Water*, 14(9), 1362.

Mishra, A. K., Upadhyay, A., Srivastava, A., & Rai, S. C. (2020). Probabilistic groundwater recharge zonation in hard rock terrain using geospatial techniques in Veniar watershed, South India. *Ecohydrology & Hydrobiology*, 20(3), 456-471.

Mogaji, K. A., & Omobude, O. B. (2017). Modeling of geoelectric parameters for assessing groundwater potentiality in a multifaceted geologic terrain, Ipinsa Southwest, Nigeria–A GIS-based GODT approach. *NRIAG Journal of Astronomy and Geophysics*, 6(2), 434-451.

Nag, S. K., & Ghosh, P. (2013). Delineation of groundwater potential zone in Chhatna Block, Bankura District, West Bengal, India using remote sensing and GIS techniques. *Environmental Earth Sciences*, 70, 2115-2127.

Saaty, T.L. (2001). *Decision Making for Leaders: The Analytic Hierarchy Process for Decisions in a Complex World*. RWS Publications, Pittsburgh, PA, USA.

Singh, L. K., Jha, M. K., & Chowdary, V. M. (2017). Multi-criteria analysis and GIS modeling for identifying prospective water harvesting and artificial recharge sites for sustainable water supply. *Journal of Cleaner Production*, 142, 1436-1456.

Thapa, R., Gupta, S., Guin, S., & Kaur, H. (2017). Assessment of groundwater potential zones using multi-influencing factor (MIF) and GIS: a case study from Birbhum district, West Bengal. *Applied Water Science*, 7, 4117-4131.

The United Nations Development Programme. (2022), The United Nations World Water Development Report 2022: Groundwater: Making the Invisible Visible; Facts and Figures.

Uc Castillo, J. L., Martínez Cruz, D. A., Ramos Leal, J. A., Tuxpan Vargas, J., Rodríguez Tapia, S. A., & Marín Celestino, A. E. (2022). Delineation of groundwater potential zones (GWPZs) in a semi-arid basin through remote sensing, GIS, and AHP approaches. *Water*, 14(13), 2138.

UN. (1967). Hydrogeologic map of Lebanon. Carte hydrogelogique du Liban au 1/100000 me, United Nations, Beyrouth, Lebanon.

Widodo, L. E., Cahyadi, T. A., Notosiswoyo, S., & Widijanto, E. (2017). Application of clustering system to analyze geological, geotechnical and hydrogeological data base according to HC-system approach.

Wondim, Y. K. (2016). Flood hazard and risk assessment using GIS and remote sensing in lower Awash sub-basin, Ethiopia. *Journal of Environment and Earth Science*, 6(9), 69-86.

Zghibi, A., Mirchi, A., Msaddek, M. H., Merzougui, A., Zouhri, L., Taupin, J. D., Chekirbane, A., Chenini, I., & Tarhouni, J. (2020). Using analytical hierarchy process and multi-influencing factors to map groundwater recharge zones in a semi-arid Mediterranean coastal aquifer. *Water*, 12(9), 2525.